Acta Cryst. (1994). D**50**, 398–403

Evidence for a Dimeric Intermediate on the Crystallization Pathway of Ribonuclease A

By Magali Jullien,* Marie-Pierre Crosio and Sylvie Baudet-Nessler

Laboratoire de Biologie Structurale, Bâtiment 433, 91405 *Orsay CEDEX, France*

and Fabienne Mérola and Jean-Claude Brochon

Laboratoire pour l'Utilisation du Rayonnement Synchrotron, Bâtiment 209*D*, 91405 *Orsay CEDEX, France*

(*Received* 19 *November* 1993; *accepted* 30 *November* 1993)

Abstract

Early steps in the crystallization process of pancreatic ribonuclease have been investigated by time-dependent fluorescence anisotropy, using a labeled protein as a fluorescent probe. Previous experiments have shown that steady-state fluorescence anisotropy is sensitive to protein–protein interactions and can be used to find new crystallization conditions. The present work describes an attempt, by means of time-resolved experiments, to detect and characterize species appearing in the early stages of the crystallization pathway. Fluorescence anisotropy decay was measured with synchrotron radiation as a light source under a variety of conditions where it is known that the solutions tend towards crystallization; the decay was analyzed by a maximum-entropy method that calculates a rotational correlation-time distribution. Fluorescence anisotropy originates in the Brownian rotatory motion of macromolecules and the values of the correlation times are related to the size and shape of different species present in the solution. In the presence of high salt concentrations, a bimodal distribution is always observed. Whereas a peak of protein monomer is still present, a second peak appears as a stable intermediate in the crystallization pathway. The correlation time of this new species varies between two and three times the correlation time of the monomer. The second peak is possibly the symmetrical dimer of the ribonuclease molecules commonly observed in all the high-salt crystal forms.

Introduction

In the last few years protein crystallization has become the limiting step on the way to determining crystallographic structures. Although, for about ten years, the protein crystallization process has been investigated using physical methods such as dynamic light scattering (Feher & Kam, 1985), the manner in which the phase transition proceeds at the molecular level has remained unclear. Crystallization is considered as a nucleated polymerization, like any condensation phenomenon occurring during the phase transition from gas to liquid. At the present time the major goal remains to understand what happens in a supersaturated solution during the prenucleation phase: how macromolecules associate and dissociate and what is the nucleus critical size, *i.e.* sufficient for subsequent crystal growth.

Fluorescence polarization techniques can be used to explore the association of proteins and study aggregation processes. The potential benefits of fluorescence methods can be realized if a suitable chromophore is inserted into the protein; the chromophore must be bound at a unique location and its insertion should not appreciably disturb the features of the protein. Moreover, only global rotational motions can be investigated if the fluorescent label is rigidly attached to the molecule and if its excited-state lifetime is of suitable duration. A fluorescent derivative of bovine pancreatic ribonuclease (RNase A) which fulfils all these conditions has been used by us previously for studying, in concentrated solutions, the effect of precipitating agents on protein interactions by steady-state fluorescence polarization (Jullien & Crosio, 1991; Crosio & Jullien, 1992). This derivative, obtained by reaction with *N*-{[(iodoacetyl)amino]ethyl}-5-napthylamine-1-sulfonic acid (1,5-IAENS), crystallizes in high-salt conditions and its structure has been determined recently at 2 Å resolution (Baudet-Nessler, Jullien, Crosio & Janin, 1993). Moreover, native RNase A (Crosio, unpublished results) and several chemical derivatives have been crystallized in similar salt conditions, *i.e.* 3 *M* CsCl and ammonium sulfate at acidic pH; they include, for example, ribonuclease S (RNase S), a

* Present address: Centre de Biochimie Structurale, Unité Mixte de Recherche C 9955, CNRS, Université Montpellier I, Faculté de Pharmacie, 15 avenue Charles Flahaut, 34060 Montpellier CEDEX 1, France.

ISSN 0907-4449

complex that consists of two proteolytic fragments of RNase A, the S peptide (residues 1–20) and S protein (residues 21–124) (Kim, Varadarajan, Wykcoff & Richards, 1992), a semi-synthetic RNase A non-covalent complex of residues 1–118 with the synthetic peptide 111–124, here called RNase A* (Martin, Doscher & Edwards, 1987; De Mel, Martin, Doscher & Edwards, 1992), and a derivative with a thymidine covalently bound to His12, called RNase T-H12 (Nachman *et al.*, 1990). The labeled protein, called AENS-RNase, looked appropriate, therefore, for studying the crystallization process of RNase A in high-salt conditions by fluorescence techniques.

In the present work, we complete our previous static experiments with fluorescence anisotropy decay. The nanosecond approach complements steady-state polarization methods since it reveals directly the rotational corrrelation time and, therefore, the presence of more than one rotational correlation time can be detected. Nanosecond fluorescence measurements can also reveal whether aggregation occurs in a very short time interval; if the association–dissociation takes longer than a few nanoseconds, *i.e.* the lifetime of the excited state, the different forms will give different relaxation times. The particle-size distribution during the prenucleation phase has been determined using a maximum-entropy method analysis. A mechanism is proposed for the nucleation process of RNase A in the presence of salts.

Theory

The decay of the polarization anisotropy $r(t)$ for a fluorescent-labeled macromolecule undergoing Brownian rotational motion depends on the shape and the volume of the macromolecule, the temperature and viscosity of the medium, and the orientation of the label with respect to the macromolecule. In the most general case, when the macromolecule has no symmetry properties at all, five exponentials appear in $r(t)$ (Tao, 1969). Since such a resolution of experimental data is difficult, one usually assumes certain well defined shapes for the macromolecules. It is particularly convenient to treat the data as if they were true ellipsoids of revolution, because the hydrodynamic properties of such bodies have been worked out in detail. Thus, for prolate and oblate ellipsoids, the decay of $r(t)$ is described by three exponentials (Rigler & Ehrenberg, 1973):

$$r(t) = A_1 \exp(-t/\theta_1) + A_2 \exp(-t/\theta_2) + A_3 \exp(-t/\theta_3),$$

where θ_1, θ_2 and θ_3 denote rotational correlation times and are related to the rotational diffusion coefficients about the major ($D_\parallel$) and minor ($D_\perp$) axes according to:

$$\theta_1 = 1/6D_\perp$$
$$\theta_2 = 1/(5D_\perp + D_\parallel)$$
$$\theta_3 = 1/(2D_\perp + 4D_\parallel).$$

Perrin's hydrodynamic equations (Perrin, 1936) allow calculation of $D_\parallel$ and $D_\perp$ as a function of the axial ratio ρ between the longitudinal axis and the equatorial axis of the ellipsoid.

The pre-exponential factors A_1, A_2 and A_3 depend on the orientation of the transition moments of the fluorophore with respect to ellipsoid axes,

$$A_1 = 0.1(3\cos^2\delta_1 - 1)(3\cos^2\delta_2 - 1)$$
$$A_2 = 1.2\sin\delta_1\cos\delta_1\sin\delta_2\cos\delta_2\cos\varepsilon$$
$$A_3 = 0.3\sin^2\delta_1\sin^2\delta_2(2\cos^2\varepsilon - 1),$$

where δ_1 is the angle subtended by the absorption transition moment of the label with respect to the symmetry axis, δ_2 the angle subtended by the emission transition moment of the label with respect to the symmetry axis, ε the angle between projections of these moments in the plane perpendicular to the revolution axis; δ_1, δ_2 and ε are related by the formula

$$\cos\omega = \cos\delta_1\cos\delta_2 + \sin\delta_1\sin\delta_2\cos\varepsilon,$$

where ω is the angle between the absorption and emission moments of the dye.

$$A_0 = A_1 + A_2 + A_3 = (3\cos^2\omega - 1)/5,$$

is the intrinsic polarization anisotropy of the fluorescent probe. In the case of our label (1,5-IAENS), $\omega = 15^\circ$ and $A_0 = 0.355$ (Van der Heide, Orbons, Gerritsen & Levine, 1991).

Materials and methods

Chemicals

All chemicals were from Sigma. RNase A (molecular weight 13680 Da) was type XII. The labeled protein was prepared as previously described (Jullien & Garel, 1981). All protein solutions were prepared by adding a constant amount (0.1 mg) of labeled protein to various quantities of RNase A dissolved into a 50 m*M* sodium cacodylate buffer, pH 5.1, with the desired salt concentration. Protein concentrations were measured by tyrosine absorbance at 278 nm. Solutions were made using bidistilled deionized water and were centrifuged just prior to experiments in order to eliminate the largest aggregates.

Crystal packing

Atomic coordinates are from the Brookhaven Protein Data Bank (Bernstein *et al.*, 1977). Crystal packing contacts and solvent-accessible surface areas

were determined as previously described (Crosio, Janin & Jullien, 1992).

Mathematical models

Molecules (monomers and polymers) were represented as ellipsoids of revolution which were constructed in the following way. Mechanical parameters of the molecule (centre of mass, principal axes and principal moments of inertia) were calculated from the atomic coordinates of the atoms (except the H atoms) constituting the molecule with the program *INERT* kindly provided by Dr. J. Janin (Orsay). The three semi-axes of an equivalent homogeneous ellipsoid of mass m were obtained from the formula

$$A = m(b^2 + c^2)/5,$$

which relies on the moment of inertia A for one principal axis and the semi-axes b and c perpendicular to this axis. In order to obtain an ellipsoid of revolution, the two closest values were replaced by their mean value; therefore, the molecular shape was assumed to be an ellipsoid of revolution characterized by its axial ratio between the longitudinal axis and the equatorial axis.

Experimental methods

Fluorescence anisotropy decay was produced using as a pulsed light the synchrotron radiation from Super-ACO (Anneau de collision d'Orsay) of LURE laboratory, Orsay, France. The excitation wavelength was set at 380 nm and the emission wavelength at 480 nm. The fluorescence-decay curves obtained by pulse techniques are convolution products of the impulse response and the excitation function; a scattering solution of colloidal silica was used to measure the excitation temporal profile. The parallel $I_{\parallel}(t)$ and perpendicular $I_{\perp}(t)$ components of the emitted light were measured by the single photoelectron counting method (Brochon, Tauc, Merola & Schoot, 1993). The fluorescence anisotropy is related to the measured components by the formula

$$r(t) = [I_{\parallel}(t) + I_{\perp}(t)]/[I_{\parallel}(t) + 2I_{\perp}(t)].$$

All the measurements were performed at 293 K.

Data analysis

Data analyses were performed on a VAX 6310 computer using maximum-entropy library *MEMSYS*2 software from MEDC Ltd, Cambridge, England (Livesey & Brochon, 1987).

Results

Comparison of packing in different high-salt crystal forms of ribonuclease

RNase A and various chemical derivatives have been crystallized from salt solutions. The crystal forms belong to trigonal space groups ($P3_121$ for RNase S, or $P3_221$ for RNase A, RNase A* and AENS-RNase), except the thymidine adduct which yields orthorhombic crystals with two protein molecules in the asymmetric unit. Comparison of crystal packing reveals a common interface in all these salt crystal forms; this interface yields a dimer with a twofold symmetry which is a crystal symmetry in the trigonal space group and a local symmetry in the orthorhombic form. The corresponding total buried surface area is about 1800 Å^2, the most extensive contact never observed in all RNase crystal packing (Crosio *et al.*, 1992). Moreover, analysis of atom content in the different packing reveals that this particular interface is enriched in non-polar groups: it contains about 64% non-polar groups, whereas 56% of the solvent-accessible area of an isolated ribonuclease molecule is constituted by non-polar groups. This interface resembles subunit interfaces in oligomeric proteins (Miller, 1989), with two main-chain to main-chain hydrogen bonds pairing residues 62–64 to 86–88, as in an anti-parallel β-sheet, repeated twice.

Shape model

As well as translational diffusion or sedimentation, rotational diffusion depends on the size and shape of macromolecules, due to frictional coefficients. However, the shape of the macromolecule is, in general, complex and cannot be determined in detail by measurements of rotational motion. The usual procedure is to approximate the true shape by a geometrical shape, such as a sphere, a rod or an ellipsoid. RNase A is a small globular protein which can be considered as an ellipsoid of revolution for interpreting its hydrodynamic properties. In such an approximation, the asymmetry of the molecule is reflected by its axial ratio. The isolated molecule and various aggregates (dimer, tetramer and hexamer) observed in space group $P3_221$, were assumed to be ellipsoids of revolution and their axial ratio determined using the procedure described above (Table 1). The monomer is well represented by a prolate ellipsoid of revolution with axes 14.5 × 14.5 × 24.4 Å. The symmetrical dimer, an association of two prolate ellipsoids, appears as an oblate ellipsoid, with axes 15.9 × 25.8 × 25.8 Å, the twofold axis being the revolution axis. The more asymmetric body is the tetramer with an axial ratio of 2.3. The hexamer resembles the monomer with semi-axes both multiplied by a factor of two.

Calculated rotational correlation times

For an ellipsoid of revolution, fluorescence anisotropy decay is the sum of three exponentials whose coefficients are weighted by the orientation of the fluorescent probe with respect to the principal axes

Table 1. *Geometrical parameters of aggregates considered as ellipsoids of revolution*

Transformations of atomic coordinates in the $P3_221$ crystal form used to generate aggregates; dimer: $y, x, 1-z$; tetramer: $y-x+1, 1-x, z+1/3$; hexamer: $1-y, x-y, z-1/3$. a = major axis; b = minor axis. The axial ratio is the ratio of the longitudinal semi-axis to the equatorial semi-axis (a/b for a prolate ellipsoid and b/a for an oblate ellipsoid). δ_1 and δ_2 are defined in the *Theory* section.

Aggregate	a (Å)	b (Å)	Axial ratio	δ_1 (°)	δ_2 (°)
Monomer	24.4	14.5	1.7	78	63
Dimer	25.8	15.9	0.6	81	85
				81	67
Tetramer	51.4	22.1	2.3	60	51
				72	58
				29	40
				22	38
Hexamer	56	30.5	1.9	74	84
				64	79
				51	67
				68	53
				60	71
				70	54

Table 2. *Calculated mean correlation times of aggregates*

The different correlation times are normalized to the correlation time θ of an equivolume sphere under the same conditions of temperature and viscosity. The harmonic mean correlation time $\langle\theta\rangle$ is given by: $A_0/\langle\theta\rangle = A_1/\theta_1 + A_2/\theta_2 + A_3/\theta_3$, where A_1, A_2 and A_3 are calculated from the values of δ_1 and δ_2 given in Table 1. For each type of aggregate, the average correlation time is normalized to the correlation time of the monomer assuming the volume of the i-mer is i times the volume of the monomer.

Aggregate	θ_1/θ	θ_2/θ	θ_3/θ	$\langle\theta\rangle/\theta$	Normalized average
Monomer	1.30	1.19	0.95	1.03	1
Dimer	1.04	1.07	1.17	1.14	
				1.13	2.20 (0.01)
Tetramer	1.75	1.45	0.96	1.29	
				1.20	
				1.50	
				1.55	5.20 (0.70)
Hexamer	1.41	1.26	0.95	1.07	
				1.07	
				1.14	
				1.12	
				1.10	
				1.10	6.40 (0.20)

of the ellipsoid. In the case of an i-mer, there are i possible orientations of the probe and therefore i different values of the harmonic mean correlation time $\langle\theta\rangle$ (Table 2). For one type of aggregate, the difference among the different orientations is at most 14%; therefore, the values are close enough for assigning one average correlation time per i-mer (Table 2).

Fluorescence and anisotropy decay of labeled RNase in the presence of salt

In the absence of salt, the fluorescence decay of AENS-RNase follows a single exponential, with a lifetime of 18 ns; the anisotropy decay also follows a single exponential, with a rotational correlation time of 7 ns at 293 K in water (Jullien, Garel, Merola & Brochon, 1986). In the presence of 3 *M* CsCl, the fluorescence lifetime remains unchanged (Fig. 1). Analysis of the anisotropy decay (Fig. 1) gives a bimodal distribution, with rotational correlation times of 7.3 (1.5) and 18.6 (3.9) ns, the fast decay corresponding to 81% of the total amplitude.

Effect of protein concentration on correlation-time distribution

The correlation-time distribution for a given salt solution (3 *M* CsCl, 10% ammonium sulfate) has been studied as a function of protein concentration (Fig. 2). For 0.2 mg ml $^{-1}$, a narrow and unique peak is observed which corresponds to the correlation time of ribonuclease monomer in such conditions of viscosity; for protein concentrations higher than 11 mg ml^{-1} (Fig. 3), a second peak appears. In such salt conditions, the ribonuclease solubility is 13 (2) mg ml^{-1}. This peak is difficult to resolve between 12 and 20 mg ml^{-1} since its contribution is less than 20%. But, for 35 mg ml^{-1}, it appears clearly (Fig. 2) with a correlation time of 29.2 (3.1) ns whereas the correlation time of the monomer is 8.7 (0.9) ns. For such a protein concentration the contribution of aggregates is 36% of the total amplitude.

Effect of salt concentration on correlation-time distribution

The correlation-time distribution has been studied as a function of salt concentration, keeping the protein concentration equal to 20 mg ml^{-1}. In the

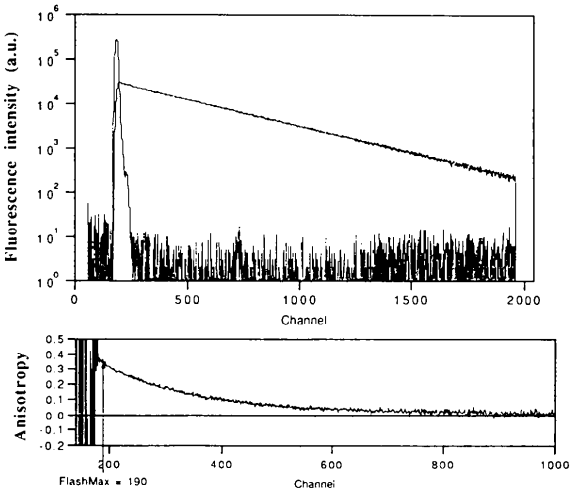

Fig. 1. Flash excitation temporal profile, fluorescence-intensity decay (top) and fluorescence-anisotropy decay (bottom) of AENS-RNase; one channel corresponds to 0.0478 ns. Excitation wavelength: 380 nm; emission wavelength: 480 nm. Total protein concentration: 20 mg ml $^{-1}$ in 3 *M* CsCl, 50 m*M* sodium cacodylate, pH 5.1, 293 K.

presence of 3 *M* CsCl, without addition of ammonium sulfate, a bimodal distribution is observed (Fig. 4); the first peak is characteristic of the monomeric ribonuclease; the second peak the correlation time of which is 2.5 times that of the monomer represents probably the dimer which contributes 19% of the total anisotropy signal. Addition of ammonium sulfate slightly shifts the second peak towards higher values (Fig. 4). For 18% saturated ammonium sulfate, the second value is 3.1 times the first one, with an amplitude of 42% (Fig. 5).

Discussion

Our major interests in protein crystallization have been concerned with what types of intermediates are present on the pathway between monomer and nucleus. Whether or not an equilibrium intermediate occurs during the polymerization depends on the stability of the intermediate relative to the initial and final states. Experimental conditions must be found where intermediates are stably populated, in order to obtain a detectable level of relative population at equilibrium. On the other hand, the characteristic time of the measurement must be fast compared with the exchange rate between intermediates. The AENS, with a fluorescence lifetime of about 20 ns, was a good tool in the search for small aggregates (up to the decamer) on the crystallization pathway of this protein.

The maximum-entropy analysis of fluorescence anisotropy decay provides the size distribution of fluorescent macromolecules in solution. In ribonuclease crystallization conditions, the correlation-time distribution cannot discriminate between more than two populations: a narrow population corresponding to ribonuclease monomers and a larger one. This second population appears to be constituted essentially by the symmetrical dimer found in all salt-grown ribonuclease crystals (Crosio, Janin & Jullien, 1992). The dimer is present only under supersaturated conditions. As soon as its concentration exceeds 20%, the probable appearance of tetramers which are not resolved from the dimer increases the correlation time of the second population. Therefore, in the presence of salt, the prenucleation phase may be described by a chain of association–dissociation reactions with a multistep equilibrium model; only monomer, dimer and tetramer are sufficiently populated to be observed. The simplest theoretical framework to interpret the experiments is to consider that an aggregate grows by successive addition of dimers:

Monomer ⟺ Dimer ⟺ Tetramer ⟺

Hexamer ... ⟺ Crystal.

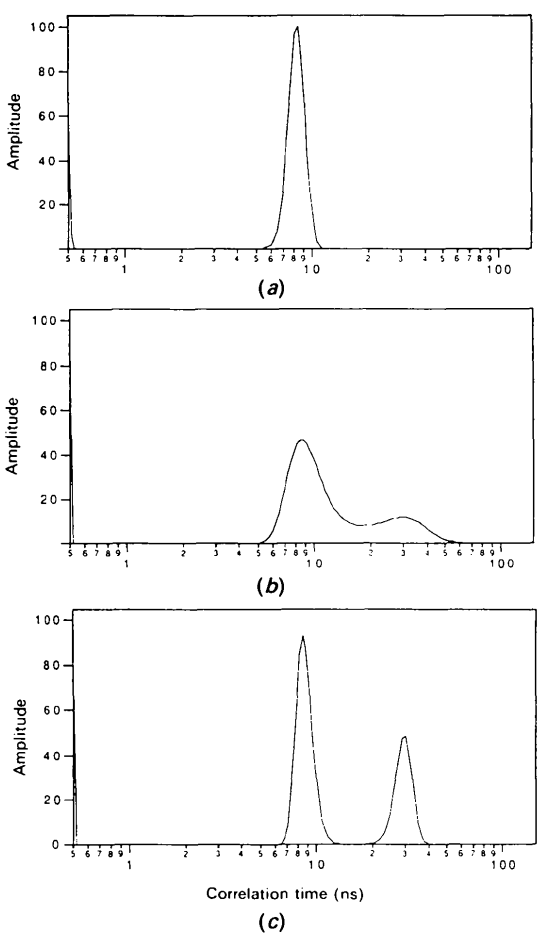

Fig. 2. Rotational correlation-time distribution in 3 *M* CsCl, 10% saturated ammonium sulfate. Protein concentration: (*a*) 0.2 mg ml $^{-1}$; (*b*) 28 mg ml^{-1}; (*c*) 35 mg ml $^{-1}$. Same buffer conditions as in the legend of Fig. 1.

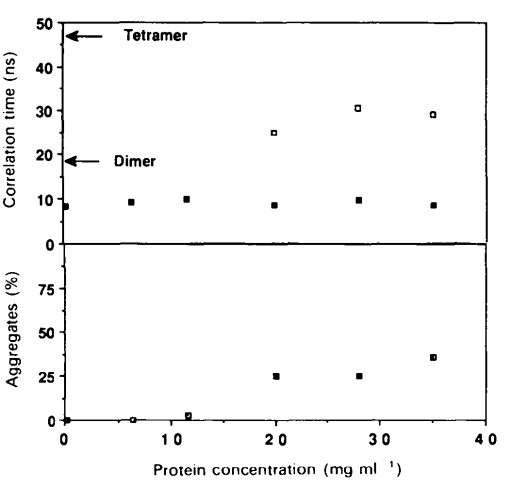

Fig. 3. Protein concentration dependence of the measured correlation times in 3 *M* CsCl, 10% saturated ammonium sulfate, 50 m*M* sodium cacodylate, pH 5.1, 293 K. ■ = short correlation time; □ = long correlation time, ⊡ = % amplitude of the slow component of the anisotropy decay.

The critical nuclear size could be a hexamer, an aggregate size which corresponds to the number of molecules in the unit cell for the trigonal space group. Such a possibility was first proposed by Ataka & Asai (1990) in the case of another protein model, hen egg-white lysozyme; by adapting a theory of protein self-assembly to the analysis of crystallization kinetics, they found that the orthorhombic crystal form can grow from preformed aggregates indentical with the unit cell of the crystal, *i.e.* from tetramers in this case.

The crystallization reaction is a growing process in which the correctly organized assembly grows. The growth is accompanied by at least two opposite contributions to the free energy: a free-energy increase caused by a decrease in mobility and a free-energy decrease due to non-specific and specific interactions between neighboring molecules including hydrophobic effects, hydrogen bonds and ion pairs. It is noticeable that, in crystals grown from salts, intermolecular contacts bury surface areas larger than those observed in crystals grown from organic solvents (Crosio, Janin & Julien, 1992; Kim *et al.*, 1992). It looks reasonable, therefore, to suppose that, in the presencce of salts, the packing driving force in the first steps of association could be a hydrophobic effect like in the folding process.

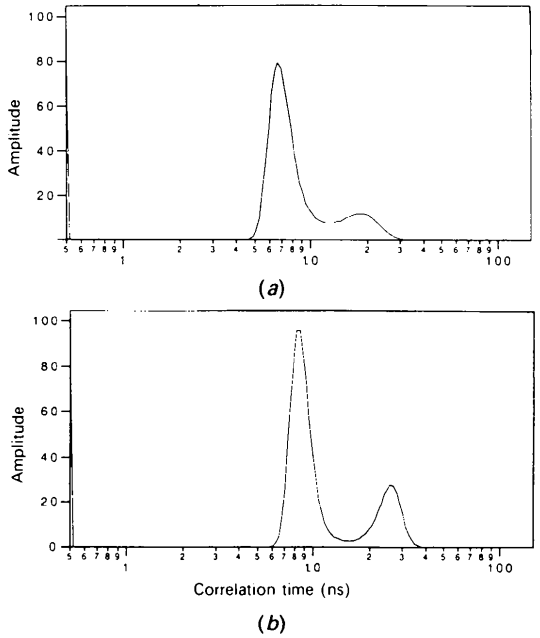

Fig. 4. Rotational correlation-time distribution for a 20 mg ml^{-1} RNase solution in 3 *M* CsCl. Ammonium sulfate concentration: (*a*) 0%; (*b*) 10%. Same buffer conditions as in the legend of Fig. 1.

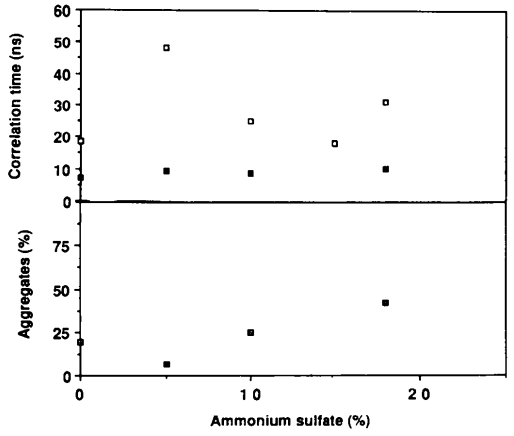

Fig. 5. Ammonium sulfate concentration dependence of the measured correlation times for a 20 mg ml^{-1} RNase solution in 3 *M* CsCl. Same symbols as in Fig. 3.

We thank the technical staff of LURE for running the synchrotron machines during the beamtime session.

References

Ataka, M. & Asai, M. (1990). *Biophys. J.* **58**, 807–811.

Baudet-Nessler, S., Jullien, M., Crosio, M.-P. & Janin, J. (1993). *Biochemistry*, **32**, 8457–8464.

Bernstein, F. C., Koetzle, T. F., Williams, G. J. B., Meyer, E. F. Jr, Brice, M. D., Rodgers, J. R., Kennard, O., Shimanouchi, T. & Tasumi, M. (1977). *J. Mol. Biol.* **112**, 535–542.

Brochon, J.-C., Tauc, P., Merola, F. & Schoot, B. M. (1993). *Anal. Chem.* **65**, 1028–1034.

Crosio, M.-P., Janin, J. & Jullien, M. (1992). *J. Mol. Biol.* **228**, 243–251.

Crosio, M.-P. & Jullien, M. (1992). *J. Cryst. Growth*, **122**, 66–70.

De Mel, V. S. J., Martin, P. D., Doscher, M. S. & Edwards, B. F. P. (1992). *J. Biol. Chem.* **267**, 247–256.

Feher, G. & Kam, Z. (1985). *Methods Enzymol.* **114**, 77–112.

Jullien, M. & Crosio, M.-P. (1991). *J. Cryst. Growth*, **110**, 182–187.

Jullien, M. & Garel, J.-R. (1981). *Biochemistry*, **20**, 7021–7026.

Jullien, M., Garel, J.-R., Merola, F. & Brochon, J.-C. (1986). *Eur. Biophys. J.* **13**, 131–137.

Kim, E. E., Varadarajan, R., Wyckoff, H. W. & Richards, F. M. (1992). *Biochemistry*, **31**, 12304–12314.

Livesey, A. K. & Brochon, J.-C. (1987). *Biophys. J.* **52**, 693–706.

Martin, P. D., Doscher, M. S. & Edwards, B. F. P. (1987). *J. Biol. Chem.* **262**, 15930–15938.

Miller, S. (1989). *Protein Eng.* **3**, 77–83.

Nachman, J., Miller, M., Gilliland, G. L., Carty, R., Pincus, M. & Wlodawer, A. (1990). *Biochemistry*, **29**, 928–937.

Perrin, F. (1936). *J. Phys. Radium (Paris)*, **7**, 1–11.

Rigler, R. & Ehrenberg, M. (1973). *Q. Rev. Biophys.* **6**, 139–199.

Tao, T. (1969). *Biopolymers*, **8**, 609–632.

Van der Heide, U. A., Orbons, B., Gerritsen, H. C. & Levine, Y. K. (1991). *Eur. Biophys. J.* **21**, 263–272.